

## A detail-preserving and flexible adaptive filter for speckle suppression in SAR imagery

JINGFENG XIAO

Department of Geography, University of North Carolina at Chapel Hill,  
Chapel Hill, NC 27599-3220, USA; e-mail: jfxiao@email.unc.edu

JING LI

Institute of Remote Sensing & GIS, Peking University, Beijing, 100871,  
P. R. China

and A. MOODY

Department of Geography, University of North Carolina at Chapel Hill,  
Chapel Hill, NC 27599-3220, USA

(Received 16 January 2001; in final form 4 February 2002)

**Abstract.** Speckle filtering and detail preservation are two key issues in speckle suppression of Synthetic Aperture Radar (SAR) imagery. Different applications may require different balances between speckle reduction and detail retention. This paper presents a detail-preserving and flexible filter. Both quantitative and qualitative criteria, including speckle reduction, edge retention, texture preservation and visual assessment, were used to evaluate the performance of this adaptive filter. One JERS-1 SAR image and three SIR-C/X-SAR images (L-HH, L-HV and C-HV) were employed in the evaluation. The results show that the proposed filter is slightly better than, or comparable to commonly used filters based on the spatial domain, such as Lee, Frost, Lee-Sigma and Gamma-Map, in terms of detail preservation. Moreover, the proposed filter can achieve a wide range of balances between speckle reduction and detail preservation, and thus is applicable in different applications, including both broad-scale interpretation or mapping and applications in which fine details and high resolution are required. Furthermore, the proposed filter requires no knowledge of speckle standard deviation, which is required in most commonly used filters.

### 1. Introduction

Synthetic Aperture Radar (SAR) imagery has become an important source of information about the Earth's surface and has been widely used in many fields, such as ecology (Ranson and Sun 1997, Kasischke *et al.* 1997), hydrology (Rott *et al.* 1996, Pope *et al.* 1997), geology (Kaupp *et al.* 1986, McHone *et al.* 1995) and oceanography (Fetterer *et al.* 1994, Nilsson and Tildesley 1995). However, SAR imagery usually exhibits a speckled appearance. Speckle degrades the quality of SAR images, and it is usually desirable to reduce speckle prior to image interpretation and further analysis (Canada Centre for Remote Sensing (CCRS) 2000). Many filtering algorithms have been developed to reduce speckle on SAR imagery (Lee

1980, 1983, Frost *et al.* 1982, Crimmins 1985, Kuan *et al.* 1987, Lopes *et al.* 1990, Martin and Turner 1993, Hagg and Sties 1994, Baraldi and Parmiggiani 1995, Aiazzi *et al.* 1997, Gagnon and Jouan 1997, Dong *et al.* 1998, Fukuda and Hirose 1998, Simard *et al.* 1998). Nevertheless, speckle suppression and detail preservation remain the two key issues in speckle filtering.

Most commonly used speckle filters have good speckle-smoothing capabilities. However, the resulting images are subject to degradation of spatial and radiometric resolution, which can result in the loss of image information (Frulla *et al.* 2000). The amount of speckle reduction desired must be balanced with the amount of detail required for the spatial scale and the nature of the particular application (CCRS 2000). For broad-scale interpretation or mapping, fine details can be ignored in many cases. Thus, significant speckle reduction and consequent loss of image details may be acceptable or appropriate in those applications (CCRS 2000). For applications in which fine details and high resolution are required, however, the detail-preserving performance of a speckle filter should be emphasized, and may be equally important as the effectiveness of speckle reduction.

The purpose of this paper is to present a detail-preserving and flexible-adaptive filter for speckle suppression of SAR imagery. This filter has several characteristics: (1) it preserves high-frequency information; (2) the balance between speckle reduction and detail preservation can be adjusted; (3) it requires no knowledge of the standard deviation of speckle noise.

## 2. Background

### 2.1. Origins and statistical properties of speckle

Speckle occurs in all types of imagery acquired from coherent imaging systems, such as laser, acoustic and SAR imagery (Kuan *et al.* 1987). This is caused by random constructive and destructive interference of the de-phased but coherent return waves scattered by the elementary scatterers within each resolution cell (Goodman 1976). Goodman (1975, 1976) gives an extensive examination of the origins and statistical properties of image speckle. The first- and second-order statistical properties of speckle are well known (Goodman 1975, Ulaby *et al.* 1986a). Fully developed speckle is characterized by a negative exponential distribution in a single-look intensity SAR image or equivalently a Rayleigh distribution in an amplitude image (Goodman 1975, 1976, Ulaby *et al.* 1986a). The probability density function of the intensity follows a Gamma distribution in multi-look images (Ulaby *et al.* 1986b). Speckle models can be incorporated in filtering techniques, and the most frequently assumed model is the multiplicative model (Durand *et al.* 1987). In most adaptive filters, which are frequently used, speckle noise is often assumed to follow a Gaussian or Gamma distribution.

### 2.2. Previous work on speckle filtering

Much work has been done on speckle filtering of SAR imagery. Filtering techniques can be grouped into multi-look processing and posterior speckle filtering techniques. Multi-look processing is applied during image formation, and this procedure averages several statistically independent looks of the same scene to reduce speckle (Porcello *et al.* 1976). A major disadvantage of this technique is that the resulting images suffer from a reduction of the ground resolution that is proportional to the number of looks  $N$  (Martin and Turner 1993). To overcome this disadvantage,

or to further reduce speckle, many posterior speckle-filtering techniques have been developed. These techniques are based on either the spatial or the frequency domain.

The Wiener filter (Walkup and Choens 1974) and other filters with criteria of minimum mean-square error (MMSE) are examples of filtering algorithms that are based upon the frequency domain (Li 1988). Recently, wavelet approaches have been used to reduce speckle in SAR images, following Mallat's (1989a, b) theoretical basis for multi-resolution analysis. Gagnon and Jouan (1997), Fukuda and Hirose (1998), Dong *et al.* (1998) and Simard *et al.* (1998) have successfully applied wavelet transformation to reduce speckle in SAR images. Gagnon and Jouan (1997) presented a Wavelet Coefficient Shrinkage (WCS) filter, which performs as well as the standard filters for low-level noise and slightly outperforms them for higher-level noise. The wavelet filter proposed by Fukuda and Hirose (1998) has satisfactory performance in both smoothing and edge preservation.

Adaptive filters based upon the spatial domain are more widely used than frequency domain filters. The most frequently used adaptive filters include Lee, Frost, Lee-Sigma and Gamma-Map. The Lee filter is based on the multiplicative speckle model, and it can use local statistics to effectively preserve edges and features (Lee 1980). The Frost filter is also based on the multiplicative speckle model and the local statistics, and it has similar performance to the Lee filter (Frost *et al.* 1982). The Lee-Sigma filter is a conceptually simple but effective alternative to the Lee filter, and Lee-Sigma is based on the sigma probability of the Gaussian distribution of image noise (Lee 1983). Lopes *et al.* (1990) developed the Gamma-Map filter, which is adapted from the Maximum A Posteriori (MAP) filter (Kuan *et al.* 1987). Lee, Frost and Lee-Sigma assume a Gaussian distribution for the speckle noise, whereas Gamma-Map assumes a Gamma distribution of speckle (Lopes *et al.* 1990). Modified versions of Gamma-Map have also been proposed (Nezry *et al.* 1991, Baraldi and Parmiggiani 1995). Nezry *et al.* (1991) combined the ratio edge detector and the Gamma-Map filter into the refined Gamma-Map algorithm. Baraldi and Parmiggiani (1995) proposed a refined Gamma-Map filter with improved geometrical adaptivity.

There are also other filters less frequently used, such as the mean filter, the median filter, the Kalman filter (Woods and Radewan 1977), the Geometric filter (Crimmins 1985), the adaptive vector linear minimum mean-squared error (LMMSE) filter (Lin and Allebach 1990), the Weighting filter (Martin and Turner 1993), the EPOS filter (Hagg and Sties 1994), the Modified  $K$ -average filter (Rao *et al.* 1995) and a texture-preserving filter (Aiazzi *et al.* 1997).

### 3. Methods

#### 3.1. Basic idea

First we consider an infinite distributed population of  $X$  (or a random variable  $X$ ) with mean  $\mu$  and variance  $\sigma^2$ . If  $\bar{X}$  is the mean of a random sample of  $n$   $X$ -observations, the probability distribution of  $\bar{X}$  has a mean of  $\mu$  and a variance of  $\sigma^2/n$  and the probability distribution of the standardized mean

$$Z = \frac{\bar{X} - \mu}{\sqrt{\sigma^2/n}} \quad (1)$$

has a mean of zero and a variance of 1 (Bradley 1976). The probability distribution of  $\bar{X}$  and  $Z$  become more and more nearly normal as  $n$  increases no matter what the shape of the original distribution of  $X$  is, and it can also be shown that the

distribution of  $\bar{X}$  and  $Z$  are also exactly normal with the means and variances already given if the original distribution of  $X$  is exactly normal (Bradley 1976).

There is usually a large number of elementary scatterers on the Earth's surface. The return signals from the scatterers can be seen as an infinite population of  $X$  with mean  $\mu$  and variance  $\sigma^2$  since the number of scatterers on the Earth's surface is sufficiently large. The return signals in a resolution cell can be seen as a sample of  $n$   $X$ -observations, and the corresponding digital number (DN) of the resolution cell can be seen as the mean of the sample. Thus, all DNs in a homogeneous image area can be considered as the means of a set of samples from a population. Therefore, the sampling distribution should be approximately normal regardless of the shape of the original distribution of  $X$ . As a consequence, it can be approximately assumed that DNs in a homogeneous image area are normally distributed (Centeno and Haertel 1995).

The DNs of the pixels corrupted by speckle and the DNs of the pixels not corrupted by speckle may follow different distributions. The DNs within a moving window (typically  $5 \times 5$  or  $7 \times 7$ ) can be considered as a sampling distribution. For the central pixel of the window, whether it is corrupted by speckle can be ascertained, to some extent, by determining whether its DN is a representative sample of the sampling distribution around that pixel. If the DN of the central pixel is a representative sample of the distribution, the DN may reflect the overall backscattering characteristics of the elementary scatters in the resolution cell. Conversely, the DN of the central pixel may follow another distribution, and hence the pixel is probably corrupted by speckle.

### 3.2. Filtering algorithm

Both the  $Z$  statistic and the  $t$  statistic can be used to determine whether a pixel is a representative sample of the sampling distribution around that pixel. The  $t$  statistic is more appropriate than the  $Z$  statistic here because the mean  $\mu$  and the standard deviation  $\sigma$  of the infinite distribution of  $X$  are unknown variables. The mean  $\bar{x}$  and the standard deviation  $\bar{\sigma}$  of all pixels within the moving window around that pixel are used to estimate the mean and the standard deviation of the sampling distribution respectively. By substituting  $\bar{x}$  and  $\bar{\sigma}$  for  $\mu$  and  $\sigma/\sqrt{n}$  in equation (1) respectively, the  $t$  statistic of the central pixel can be expressed as (Centeno and Haertel 1995)

$$T = \frac{x_0 - \bar{x}}{\bar{\sigma}} \quad (2)$$

where  $T$  is the  $t$  statistic value, and  $x_0$  is the DN of the central pixel.  $T$  is normalized to the interval  $[0, 1]$ , and the normalized value  $T_N$  is expressed as

$$T_N = \frac{T - T_{\min}}{T_{\max} - T_{\min}} \quad (3)$$

where  $T_{\max}$  and  $T_{\min}$  are the maximum and minimum  $t$  statistic values in the image, respectively, and absolute values are used for  $T$ ,  $T_{\max}$  and  $T_{\min}$ . The normalized value  $T_N$  provides an inverse measure for the likelihood that the central pixel follows the sampling distribution around that pixel. The lower the  $T_N$  value, the higher the likelihood that the central pixel belongs to the distribution of the DN values within the window and, thus, that it is not influenced by speckle.

The probability  $p$  that the central pixel follows the distribution of the DN values

within the window around that pixel can be expressed as

$$p = 1 - T_N \quad (4)$$

The higher the  $p$  value, the higher the probability that the central pixel follows the distribution of the DNs within the window.

The new adaptive filter takes the following form

$$\hat{x} = kx_0 + (1 - k)\bar{x} \quad (5)$$

where  $x_0$  is the original DN of the central pixel within a moving window,  $\bar{x}$  is the mean of all DNs within that window,  $\hat{x}$  represents the DN of the central pixel in the filtered image, and  $k$  is the probability that the central pixel is corrupted by speckle noise. The general form of this filter is similar to that of Lee (1980), since both filters replace the DN of the central pixel with a weighted average between its original DN and the local mean. However, these two filters are significantly different in that they are based on different assumptions and they use different approaches to determine the value of the weight parameter  $k$ . The Lee filter uses the local statistics and speckle standard deviation to determine  $k$ , whereas the proposed filter makes use of the likelihood that the central pixel follows the sampling distribution surrounding that pixel, and two adjustable parameters to determine  $k$ . The determination of  $k$  in the proposed filter can be expressed as

$$k = \begin{cases} 0, & 0 \leq p \leq a \\ \frac{p-a}{b-a}, & a < p < b \\ 1, & b \leq p \leq 1 \end{cases} \quad (6)$$

where  $k$  is the probability that the central pixel is corrupted by speckle,  $a$  and  $b$  are two adjustable parameters ( $0 \leq a \leq b \leq 1$ ).

An intuitive explanation to the filter is that whether strong or weak smoothing would be applied to a pixel depends on  $p$ . If  $p$  approaches 0, the pixel will be considered as speckle and its DN will be replaced by the local mean  $\bar{x}$ ; if  $p$  approaches 1, then the pixel will be considered free of speckle and its DN will remain unchanged. As shown in equation (6), we introduce two parameters  $a$  and  $b$  to determine  $k$ , so that different balances between speckle reduction and detail preservation can be achieved by adjusting  $a$  and  $b$ . As shown in equations (5) and (6), if  $p$  is less than or equal to  $a$ , then  $k$  is equal to 0, and the DN value of the central pixel is replaced by the local mean  $\bar{x}$ . If  $p$  is greater than or equal to  $b$ , then  $k$  is equal to 1, and the DN value of the central pixel will remain unchanged; otherwise, the DN value of the central pixel is replaced by a weighted average between its original DN value and the local mean  $\bar{x}$ .

### 3.3. Evaluation

The performance of the proposed filter was evaluated and compared with several of the most widely used adaptive filters based on the spatial domain, including the Lee, Frost, Lee-Sigma and Gamma-Map filters. For the Gamma-Map filter, only the most commonly used algorithm (Lopes *et al.* 1990) was used. The modified versions of Gamma-Map (Nezry *et al.* 1991, Baraldi and Parmiggiani 1995) were not used here, because they are neither widely used nor readily available in commercial

softwares. ERDAS Imagine was used for the comparisons. This image processing system incorporates the above-mentioned, commonly used speckle filters. A JERS-1 SAR image and three SIR-C/X-SAR images (L, L and C band) with HH, HV and HV polarizations were used.

Both quantitative and qualitative criteria, including speckle reduction, edge retention, texture preservation and visual assessment, were used to evaluate the performance of the proposed filter.

### 3.3.1. Speckle reduction

Equivalent Number of Looks (ENL) is often used to estimate the speckle noise level in a SAR image (Gagnon and Jouan 1997). ENL is the mean-to-standard-deviation ratio, which is a measure of the signal-to-noise ratio and is often calculated in a homogeneous image area (Gagnon and Jouan 1997). ENL is used to measure the degree of speckle reduction in this study. The higher the ENL value, the stronger the speckle reduction.

### 3.3.2. Edge retention

The ENL can only be used to measure the speckle-smoothing capability of filters, because it carries no information on the loss of high-frequency information (Gagnon and Jouan 1997). Thus, Robert's edge detector (Peli and Malah 1982) was employed to measure the edge-preserving performances of the commonly used filters and the new filter.

### 3.3.3. Texture preservation

Texture information in remotely sensed imagery, especially SAR images, has received increasing attention in image interpretation and classification. The texture-preserving capability, therefore, should play an important role in measuring the performance of a speckle filter. A second-order texture operator, Variance (Irons and Petersen 1981), was used to measure the retention of texture information in the original and the filtered images.

## 4. Results and discussions

### 4.1. Effects of $a$ and $b$ on filter performance

Figure 1 (a) illustrates that the proposed filter can achieve a wide range of speckle-smoothing effects by adjusting the values of  $a$  and  $b$ . At the bottom-left corner ( $a=0.00$ ,  $b=0.00$ ) the filter has the weakest smoothing performance. In that case, all DN values remain unchanged. The speckle-smoothing effect becomes stronger with the increase of one of the two parameters  $a$  and  $b$  when the other one of  $a$  and  $b$  is constant. The proposed filter achieves stronger smoothing effect with the simultaneous increase of  $a$  and  $b$ . At the top-right corner ( $a$  and  $b$  approach 1.00) the filter has the strongest smoothing effect. In this case, the proposed filter is equivalent to the mean filter, because the DN value of any central pixel is replaced by the local mean of the window around that pixel.

Figure 1 (b) and (c) shows the influences of  $a$  and  $b$  on edge retention and texture preservation. At the top-right corner ( $a$  and  $b$  approach 1.00) the proposed filter achieves the lowest effects of both edge and texture retention, and in this case the proposed filter is equivalent to the mean filter. At the bottom-left corner ( $a=0.00$ ,  $b=0.00$ ) all DN values remain unchanged. The proposed filter achieves increasing performance of both edge and texture retention with the decrease of  $a$  and  $b$  from 1.00 to 0.00.

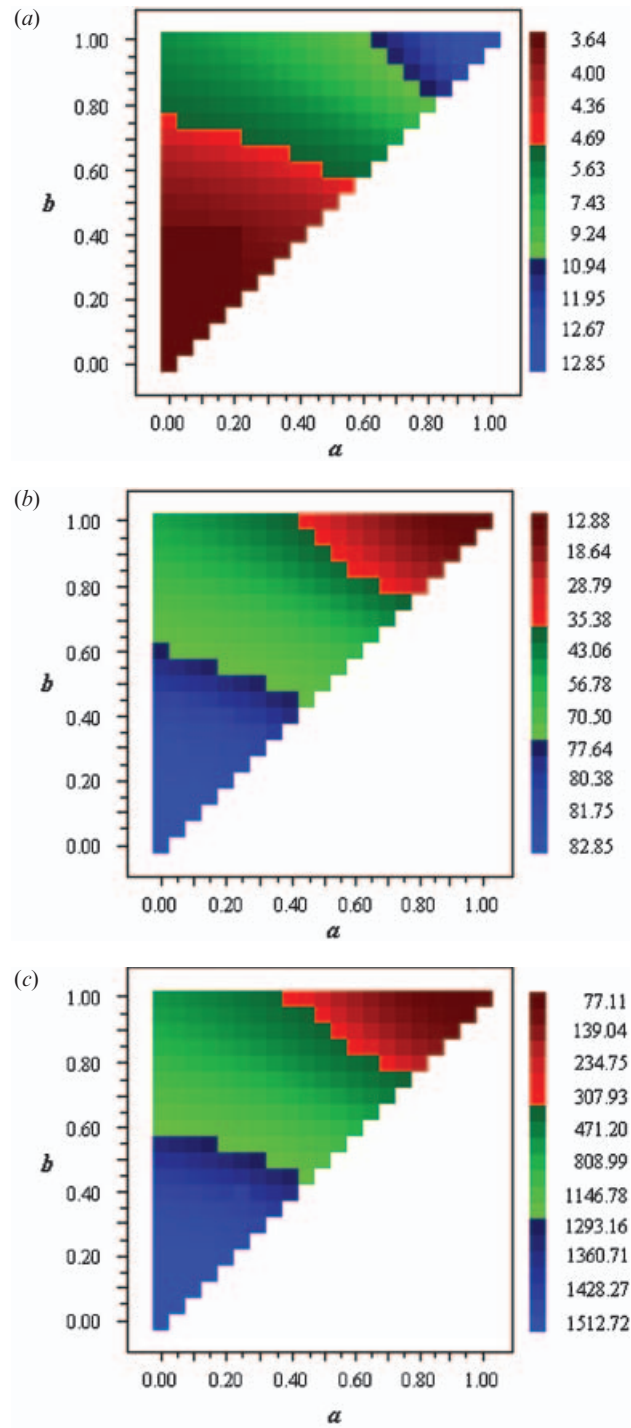


Figure 1. The influences of  $a$  and  $b$  on the performance of the proposed filter: (a) speckle-smoothing performance, measured by Equivalent Number of Looks (ENL); (b) the performance of edge retention, measured by Robert's edge detector; (c) texture preservation, measured by Variance texture operator.

Figure 2 shows the original JERS-1 image and the images filtered with the Lee, Frost, Lee-Sigma, Gamma-Map and the proposed filter. Figures 3, 4 and 5, respectively, illustrate the original and filtered L-HH, L-HV and C-HV SIR-C/X-SAR images.

#### 4.2. Speckle reduction

The ENL values of the original JERS-1 SAR image and the filtered images are given in table 1. Of the four commonly used filters, Gamma-Map and Lee have higher speckle-smoothing capabilities than Frost and Lee-Sigma. The ENL values of the proposed filter vary from 5.40 to 12.14, and thus the proposed filter can achieve a wide range of speckle-smoothing effects. The strongest smoothing effect of the proposed filter ( $a=0.8$ ,  $b=0.95$ ) is almost comparable to that of Gamma-Map.

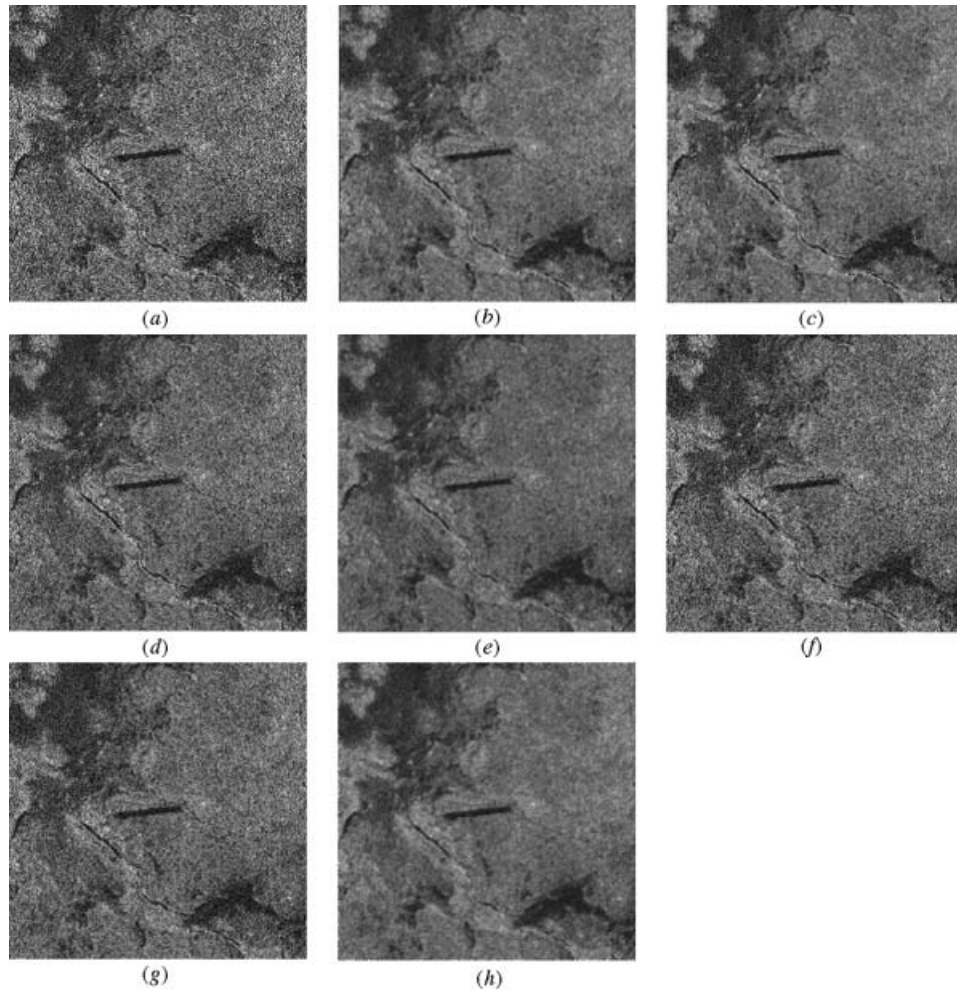


Figure 2. The original and filtered JERS-1 SAR images: (a) the original image; (b) the Lee filter; (c) the Frost filter; (d) the Lee-Sigma filter; (e) the Gamma-Map filter; (f) the proposed filter ( $a=0.20$ ,  $b=0.80$ ); (g) the proposed filter ( $a=0.40$ ,  $b=0.80$ ); and (h) the proposed filter ( $a=0.80$ ,  $b=0.90$ ).

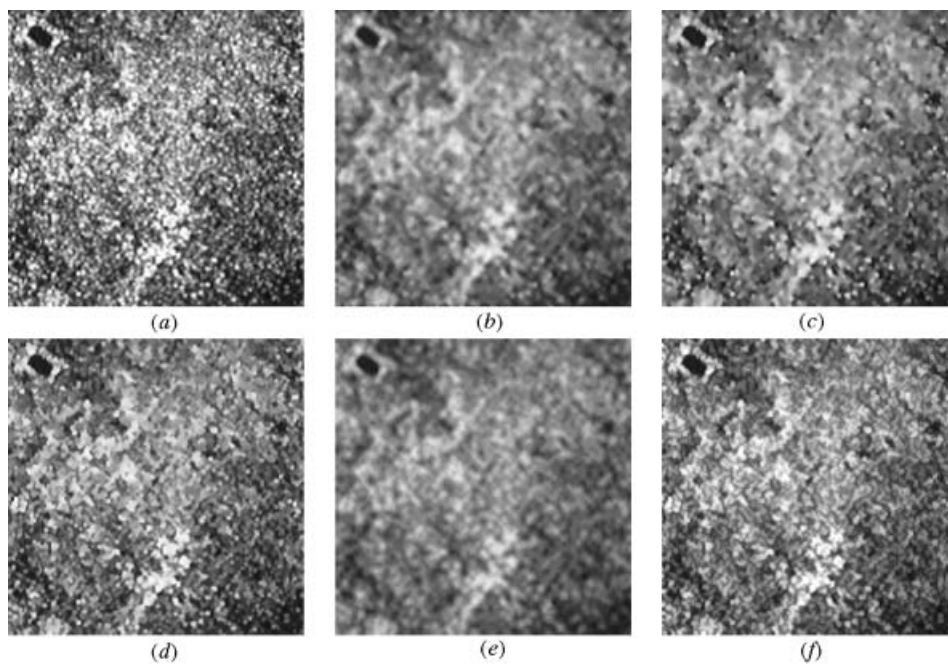


Figure 3. The original and filtered L-HH SIR-C/X-SAR images: (a) the original image; (b) the Lee filter; (c) the Frost filter; (d) the Lee-Sigma filter; (e) the Gamma-Map filter; and (f) the proposed filter ( $a=0.20$ ,  $b=0.80$ ).

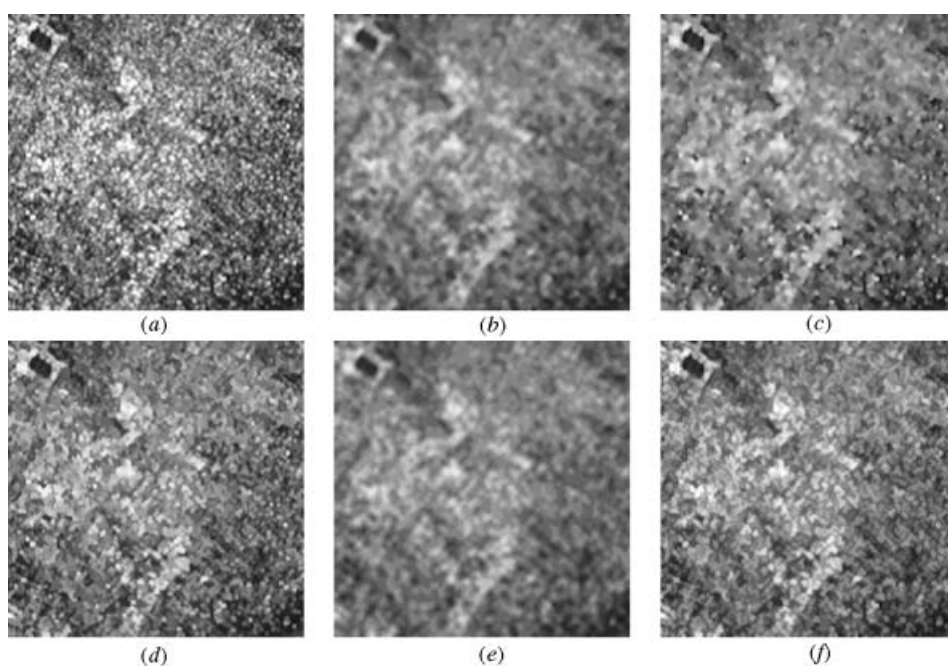


Figure 4. The original and filtered L-HV SIR-C/X-SAR images: (a) the original image; (b) the Lee filter; (c) the Frost filter; (d) the Lee-Sigma filter; (e) the Gamma-Map filter; (f) the proposed filter ( $a=0.20$ ,  $b=0.80$ ).

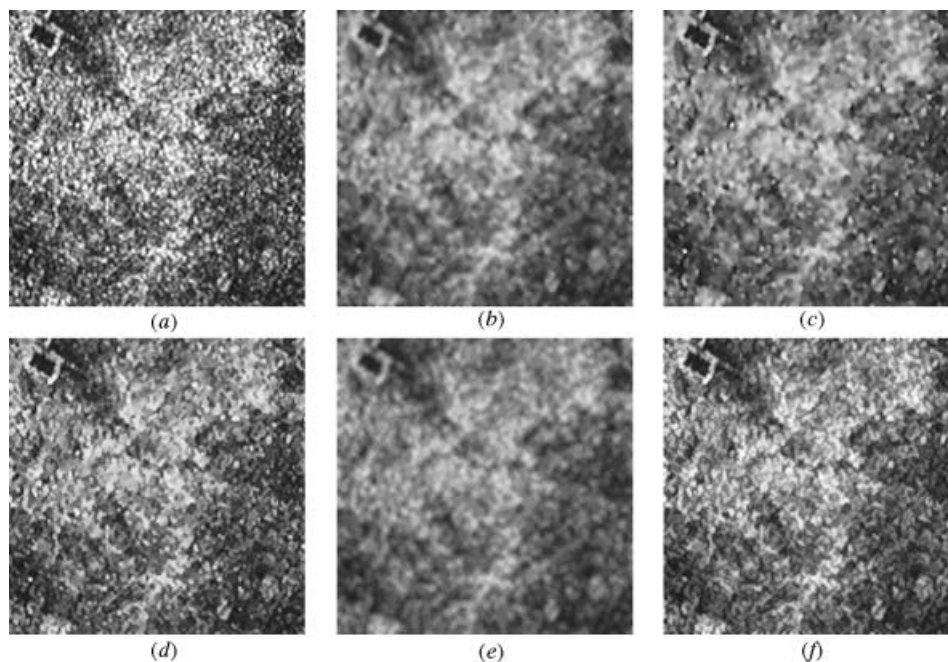


Figure 5. The original and filtered C-HV SIR-C/X-SAR images: (a) the original image; (b) the Lee filter; (c) the Frost filter; (d) the Lee-Sigma filter; (e) the Gamma-Map filter; (f) the proposed filter ( $a=0.20$ ,  $b=0.80$ ).

Table 1. Comparison of ENL, Robert's Edge Operator and Variance Texture Operator of the original JERS-1 image and the images filtered using the Lee, Frost, Lee-Sigma, Gamma-Map and the proposed filter. A  $5 \times 5$  window was used in all cases.

Image	ENL	Robert's Edge Operator	Variance Texture Operator
Original image	3.64	82.85	1512.83
Lee	11.07	19.28	145.07
Frost	9.40	23.79	244.36
Lee-Sigma			
(cvm = 0.5)*	6.04	50.96	653.51
(cvm = 1.0)	7.81	31.10	284.67
(cvm = 2.0)	9.13	24.03	199.48
Gamma-Map	12.54	14.83	91.15
New filter			
( $a=0.20$ , $b=0.80$ )	5.40	60.89	793.20
( $a=0.40$ , $b=0.80$ )	6.04	54.17	636.98
( $a=0.60$ , $b=0.80$ )	7.65	40.64	380.14
( $a=0.80$ , $b=0.95$ )	12.14	16.37	99.41

\*cvm: coefficient of variation multiplier.

The ENL values for the original and filtered L-HH, L-HV and C-HV SIR-C/X-SAR images are given in tables 2, 3 and 4, respectively. As for the JERS-1 image, Gamma-Map and Lee achieve stronger speckle-smoothing effects than Frost and Lee-Sigma. The proposed filter achieves a slightly stronger smoothing capability than

Table 2. Comparison of ENL, Robert's Edge Operator and Variance Texture Operator of the original L-HH SIR-C/X-SAR image and the images filtered using Lee, Frost, Lee-Sigma, Gamma-Map and the proposed filter. A  $5 \times 5$  window was used in all cases.

Image	ENL	Robert's Edge Operator	Variance Texture Operator
Original image	4.74	66.72	1557.86
Lee	8.87	22.76	321.22
Frost	7.19	32.48	601.14
Lee-Sigma			
(cvm = 0.5)	5.65	47.34	1007.74
(cvm = 1.0)	6.57	32.12	558.54
(cvm = 2.0)	7.83	25.29	375.41
Gamma-Map	9.56	21.44	268.83
New filter			
( $a=0.10, b=0.80$ )	5.88	48.64	909.34
( $a=0.20, b=0.80$ )	5.90	46.80	912.32
( $a=0.40, b=0.80$ )	6.57	40.51	631.46
( $a=0.60, b=0.80$ )	7.68	32.75	421.72
( $a=0.80, b=0.90$ )	9.78	21.40	239.36

Table 3. Comparison of ENL, Robert's Edge Operator and Variance Texture Operator of the original L-HV SIR-C/X-SAR image and the images filtered using Lee, Frost, Lee-Sigma, Gamma-Map and the new filter. A  $5 \times 5$  window was used in all cases.

Image	ENL	Robert's Edge Operator	Variance Texture Operator
Original image	6.78	54.43	1035.16
Lee	12.24	18.45	214.72
Frost	9.87	27.04	422.97
Lee-Sigma			
(cvm = 0.5)	8.11	38.82	681.38
(cvm = 1.0)	9.41	26.44	392.94
(cvm = 2.0)	10.98	20.43	253.84
Gamma-Map	12.72	17.97	196.40
New filter			
( $a=0.10, b=0.80$ )	8.85	36.97	535.01
( $a=0.20, b=0.80$ )	9.18	35.01	480.60
( $a=0.40, b=0.80$ )	10.17	30.23	359.59
( $a=0.60, b=0.80$ )	11.64	24.52	251.89
( $a=0.80, b=0.90$ )	13.40	17.37	166.35

Gamma-Map and Lee, and, again, produces a wide range of speckle-smoothing effects.

#### 4.3. Edge retention

Results show that Lee, Frost and Gamma-Map have similar edge-preserving capabilities for all image types (tables 1–4). Lee-Sigma and the proposed filter can both preserve edges better than Lee, Frost or Gamma-Map, but only at the cost of slightly lower speckle-smoothing effects. The edge-preserving effects of these two filters are comparable to those of Lee, Frost and Gamma-Map when the compared filters have equivalent smoothing effects. Both Lee-Sigma and the proposed filter

Table 4. Comparison of ENL, Robert's Edge Operator and Variance Texture Operator of the original C-HV SIR-C/X-SAR image and the images filtered using Lee, Frost, Lee-Sigma, Gamma-Map and the new filter. A  $5 \times 5$  window was used in all cases.

Image	ENL	Robert's Edge Operator	Variance Texture Operator
Original image	4.11	67.63	1545.07
Lee	7.42	21.87	291.41
Frost	6.21	31.57	548.29
Lee-Sigma			
( $cvm = 0.5$ )	4.81	48.07	988.07
( $cvm = 1.0$ )	5.59	31.51	515.73
( $cvm = 2.0$ )	6.66	24.46	340.91
Gamma-Map	7.94	20.48	241.84
New filter			
( $a = 0.10, b = 0.80$ )	5.25	45.01	762.63
( $a = 0.20, b = 0.80$ )	5.40	42.51	680.61
( $a = 0.40, b = 0.80$ )	5.88	36.38	499.50
( $a = 0.60, b = 0.80$ )	6.74	29.14	338.74
( $a = 0.80, b = 0.90$ )	8.04	20.01	212.22

can have different or adjustable edge-preserving performances. The Roberts' edge operator values of the proposed filter are slightly higher than those of Lee-Sigma when the two filters have equivalent ENL values. Thus, the edge-preserving performance of the new filter is slightly better than, or comparable to, those of the commonly used speckle filters, such as Lee, Frost, Gamma-Map and Lee-Sigma.

#### 4.4. Texture preservation

Lee-Sigma and the proposed filter both retain texture better than Lee, Frost and Gamma-Map, but at the cost of relatively lower smoothing effects (tables 1–4). Moreover, the texture-preserving performances of the two filters are comparable to those of Lee, Frost and Gamma-Map when the compared filters have equivalent smoothing effects. Again, the proposed filter can achieve a wide range of texture-preserving effects.

#### 4.5. Visual assessment

As shown in figure 2, the proposed filter (figure 2 (*f*) and (*g*)) can retain fine details better than the commonly used filters (figure 2 (*a*)–(*e*)). The proposed filter (figure 2 (*h*)) can also achieve comparable speckle-smoothing effects with the commonly used filters. Thus, the proposed filter accommodates different balances between speckle reduction and detail retention (figure 2 (*f*)–(*h*)). The original and filtered L-HH, L-HV and C-HV SIR-C/X-SAR images are shown in figures 3, 4 and 5. These images also show that the proposed filter is slightly better than the commonly used filters in terms of preserving details. The proposed filter is also effective in smoothing speckles. Furthermore, the proposed filter produces visually natural images.

### 5. Conclusions

Speckle reduction and detail retention are two key issues in speckle suppression of SAR imagery. The nature and the spatial scale of the application determine how big or how small features should appear and how much detail should be preserved

in the filtered image. Different applications may require different balances between speckle reduction and detail retention. For those applications in which full resolution and fine details are required, the detail-preserving capabilities of speckle filters should be emphasized and may be as important as the effectiveness of speckle reduction.

Both quantitative and qualitative criteria, including speckle smoothing, edge retention, texture preservation and visual assessment, were used to evaluate the performance of the proposed filter. Different types of images, including a JERS-1 image and three SIR-C/X-SAR images (L-HH, L-HV and C-HV) were employed for this purpose. The evaluation and comparison show that the proposed filter is slightly better than, or comparable to, several commonly used filters, including Lee, Frost, Lee-Sigma and Gamma-Map, in terms of speckle suppression and detail preservation. Moreover, the proposed filter can achieve different balances between speckle reduction and detail preservation by adjusting the parameters  $a$  and  $b$ . Thus, the proposed filter can be applied in different applications, including both broad-scale interpretation or mapping and those applications that require high resolution and fine details. Furthermore, the knowledge of speckle standard deviation is required in most commonly used speckle filters, and the estimation of speckle standard deviation is not a straightforward task (Frulla *et al.* 2000). The proposed filter requires no knowledge of speckle standard deviation.

### Acknowledgments

The authors would like to take this opportunity to thank Jiazhong Yu, Institute of Remote Sensing & GIS, Peking University, Beijing, P. R. China, for providing the JERS-1 SAR image. The SIR-C/X-SAR images were kindly provided by NASA/Jet Propulsion Laboratory/California Institute of Technology. We are also grateful to one anonymous reviewer for valuable comments on the manuscript.

### References

- AIAZZI, B., ALPARONE, L., BARONTI, S., and CARLA, R., 1997, Adaptive texture-preserving filtering of multitemporal ERS-1 images. *Proceedings of IGARSS' 97, IEEE International Geoscience and Remote Sensing Symposium, 3–8 August 1997* (Singapore: IGARSS), pp. 2066–2068.
- BARALDI, A., and PARMIGGIANI, F., 1995, A refined Gamma Map SAR speckle filter with improved geometrical adaptivity. *IEEE Transactions on Geoscience and Remote Sensing*, **33**, 1245–1257.
- BRADLEY, J. V., 1976, *Probability, Decisions, Statistics* (New Jersey: Prentice-Hall).
- CCRS, 2000, *Fundamentals of Remote Sensing Tutorial* ([www.ccrs.nrcan.gc.ca/ccrs/eduref/tutorial/indexe.html](http://www.ccrs.nrcan.gc.ca/ccrs/eduref/tutorial/indexe.html)).
- CENTENO, J. A. S., and HAERTEL, V., 1995, Adaptive low-pass fuzzy filter for noise removal. *Photogrammetric Engineering & Remote Sensing*, **61**, 1267–1272.
- CRIMMINS, T. R., 1985, Geometric filter for speckle reduction. *Applied Optics*, **24**, 1438–1443.
- DONG, Y., FORSTER, B. C., MILNE, A. K., and MORGAN, G. A., 1998, Speckle suppression using recursive wavelet transforms. *International Journal of Remote Sensing*, **19**, 317–330.
- DURAND, J. M., GIMONET, B. J., and PERBOS, J. R., 1987, SAR data filtering for classification. *IEEE Transactions on Geoscience and Remote Sensing*, **25**, 629–637.
- FETTERER, F. M., GINERIS, D., and KWOK, R., 1994, Sea ice type map from Alaska synthetic aperture radar facility imagery: an assessment. *Journal of Geophysical Research*, **99**, 22443–22458.
- FROST, V. S., STILES, J. A., SCHANMUGAN, K. S., and HOLZMAN, J. C., 1982, A model for radar images and its application to adaptive digital filtering of multiplicative noise. *IEEE Transactions on Pattern Analysis and Machine Intelligence*, **4**, 157–166.
- FRULLA, L. A., MILOVICH, J. A., and GAGLIARDINI, D. A., 2000, Automatic computation of

- speckle standard deviation in SAR images. *International Journal of Remote Sensing*, **21**, 2883–2899.
- FUKUDA, S., and HIROSAWA, H., 1998, Suppression of speckle in synthetic aperture radar images using wavelets. *International Journal of Remote Sensing*, **19**, 507–519.
- GAGNON, L., and JOUAN, A., 1997, Speckle filtering of SAR images—a comparative study between complex-wavelet-based and standard filters. *Proceedings of SPIE Wavelet Applications in Signal and Image Processing, 1997*, SPIE volume 3169, pp. 80–91.
- GOODMAN, J. W., 1975, Statistical properties of laser speckle patterns. In *Laser Speckle and Related Phenomena*, edited by J. C. Dainty (Berlin: Springer-Verlag), pp. 9–75.
- GOODMAN, J. W., 1976, Some fundamental properties of speckle. *Journal of the Optical Society of America*, **66**, 1145–1150.
- HAGG, W., and STIES, M., 1994, Efficient speckle filtering of SAR images. *Proceedings of IGARSS' 94, 1994* (California: IGARSS), pp. 2140–2142.
- IRONS, J. R., and PETERSEN, G. W., 1981, Texture transforms of remote sensing data. *Remote Sensing of Environment*, **11**, 359–370.
- KASISCHKE, E. S., MELACK, J. M., and DOBSON, M. C., 1997, The use of imaging radars for ecological applications—a review. *Remote Sensing of Environment*, **59**, 141–156.
- KAUPP, V. H., GADDIS, L. R., MOUGINIS-MARK, P. J., DERRYBERRY, B. A., MACDONALD, H. C., and WAITE, W. P., 1986, Preliminary analysis of SIR-B radar data for recent Hawaii lava flows. *Remote Sensing of Environment*, **20**, 283–290.
- KUAN, D. T., SAWCHUK, A. A., STRAND, T. C., and CHAVEL, P., 1987, Adaptive restoration of images with speckle. *IEEE Transactions on Acoustics, Speech, and Signal Processing*, **35**, 373–383.
- LEE, J. S., 1980, Digital image enhancement and noise filtering by use of local statistics. *IEEE Transactions on Pattern Analysis and Machine Intelligence*, **2**, 165–168.
- LEE, J. S., 1983, Digital image smoothing and the sigma filter. *Computer Vision, Graphics and Image Processing*, **24**, 255–269.
- LI, C., 1988, Two adaptive filters for speckle reduction in SAR images by using the variance ratio. *International Journal of Remote Sensing*, **9**, 641–653.
- LIN, Q., and ALLEBACH, J. P., 1990, Combating speckle in SAR images: vector filtering and sequential classification based on a multiplicative noise model. *IEEE Transactions on Geoscience and Remote Sensing*, **28**, 647–653.
- LOPES, A., NEZRY, E., TOUZI, R., and LAUR, H., 1990, Maximum a posteriori speckle filtering and first order texture models in SAR images. *Proceedings of IGARSS' 90, May 1990*, vol. 3 (Maryland: IGARSS), pp. 2409–2412.
- MALLAT, S. G., 1989a, A theory for multiresolution signal decomposition: the wavelet representation. *IEEE Transactions on Pattern Analysis and Machine Intelligence*, **11**, 674–693.
- MALLAT, S. G., 1989b, Multifrequency channel decomposition of images and wavelet models. *IEEE Transactions on Acoustics, Speech, and Signal Processing*, **37**, 2091–2110.
- MARTIN, F. J., and TURNER, R. W., 1993, SAR speckle reduction by weighted filtering. *International Journal of Remote Sensing*, **14**, 1759–1774.
- MCHONE, J. F., BLUMBERG, D. G., GREELEY, R., and UNDERWOOD, J. R., 1995, Space shuttle radar images of terrestrial impact structures—SIR-C/X-SAR. *Meteoritics*, **30**, 543.
- NEZRY, E., LOPES, A., and TOUZI, R., 1991, Detection of structural and textural features for SAR images filtering. *Proceedings of IGARSS' 91, June 1991*, vol. 3 (Helsinki: IGARSS), pp. 2169–2172.
- NILSSON, C. S., and TILDESLEY, P. C., 1995, Imaging of oceanic features by ERS-1 synthetic aperture radar. *Journal of Geophysical Research*, **100**, 953–967.
- PELL, T., and MALAH, D., 1982, A study of edge detection algorithms. *Computer Graphics and Image Processing*, **20**, 1–21.
- POPE, K. O., REJMANKOVA, E., PARIS, J. F., and WOODRUFF, R., 1997, Monitoring seasonal flooding cycles in marshes of the Yucatan Peninsula with SIR-C Polarimetric Radar Imagery. *Remote Sensing of Environment*, **59**, 157–166.
- PORCELLO, L. J., MASSEY, N. G., INNES, R. B., and MARKS, J. M., 1976, Speckle reduction in synthetic radars. *Journal of the Optical Society of America*, **66**, 1305–1311.
- RANSON, K. J., and SUN, G., 1997, An evaluation of AIRSAR and SIR-C/X-SAR images for mapping northern forest attributes in Maine, USA. *Remote Sensing of Environment*, **59**, 203–222.

- RAO, P. V. N., VIDYADHAR, M. S. R. R., RAO, T. C. M., and VENKATARATNAM, L., 1995, An adaptive filter for speckle suppression in synthetic aperture radar images. *International Journal of Remote Sensing*, **16**, 877–889.
- ROTT, H., SKVARCA, P., and NAGLER, T., 1996, Rapid collapse of northern Larsen ice shelf, Antarctica. *Science*, **271**, 788–792.
- SIMARD, M., DEGRANDI, G., THOMSON, P. B., and BENIE, G. B., 1998, Analysis of speckle noise contribution on wavelet decomposition of SAR images. *IEEE Transactions on Geoscience and Remote Sensing*, **36**, 1953–1962.
- ULABY, F. T., MOORE, R. K., and FUNG, A. K., 1986a, *Microwave Remote Sensing: Active and Passive III: From Theory to Applications* (Norwood: Artech House).
- ULABY, F. T., KOUYAFE, F., BRISCO, B., and WILLIAMS, L., 1986b, Textural information in SAR images. *IEEE Transactions on Geoscience and Remote Sensing*, **24**, 235–245.
- WALKUP, J. F., and CHOENS, R. C., 1974, Image processing in signal dependent noise. *Optical Engineering*, **13**, 250–266.
- WOODS, J. W., and RADEWAN, C. H., 1977, Kalman filtering in two dimensions. *IEEE Transactions on Information Theory*, **23**, 473–482.